Effects of mass distribution on the mechanics of level trotting in dogs

David V. Lee*, Eric F. Stakebake, Rebecca M. Walter and David R. Carrier

Department of Biology, University of Utah, 257 South 1400 East, Salt Lake City, UT 84112-0840, USA

*Author for correspondence at present address: Concord Field Station, Department of Organismic and Evolutionary Biology,
Harvard University, Bedford, MA 01730, USA (e-mail: dlee@oeb.harvard.edu)

Summary

The antero–posterior mass distribution of quadrupeds varies substantially amongst species, yet the functional implications of this design characteristic remain poorly understood. During trotting, the forelimb exerts a net braking force while the hindlimb exerts a net propulsive force. Steady speed locomotion requires that braking and propulsion of the stance limbs be equal in magnitude. We predicted that changes in body mass distribution would alter individual limb braking–propulsive force patterns and we tested this hypothesis by adding 10% body mass near the center of mass, at the pectoral girdle, or at the pelvic girdle of trotting dogs. Two force platforms in series recorded fore- and hindlimb ground reaction forces independently. Vertical and fore–aft impulses were calculated by integrating individual force–time curves and Fourier analysis was used to quantify the braking–propulsive (b–p) bias of the fore–aft force curve. We predicted that experimental manipulation of antero–posterior mass distribution would (1) change the fore–hind distribution of vertical impulse when the limb girdles are loaded, (2) decrease the b–p bias of the experimentally loaded limb and (3) increase relative contact time of the experimentally loaded limb, while (4) the individual limb mean fore–aft forces (normalized to body weight + added weight) would be unaffected. All four of these results were observed when mass was added at the pelvic girdle, but only 1, 3 and 4 were observed when mass was added at the pectoral girdle. We propose that the observed relationship between antero–posterior mass distribution and individual limb function may be broadly applicable to quadrupeds with different body types. In addition to the predicted results, our data show that the mechanical effects of adding mass to the trunk are much more complex than would be predicted from mass distribution alone. Effects of trunk moments due to loading were evident when mass was added at the center of mass or at the pelvic girdle. These results suggest a functional link between appendicular and axial mechanics *via* action of the limbs as levers.

Key words: locomotion, running, dog, *Canis*, force, braking, propulsion, center of mass, limb, trunk.

Introduction

The function of individual limbs is difficult to assess in running quadrupeds. Not only are the limbs in different positions with respect to the center of mass, they also interact simultaneously with the substrate. During steady speed trotting, forelimbs typically exert a net braking force, while hindlimbs exert a net propulsive force. A common generalization that fore- and hindlimbs of quadrupeds exert similar forces (Alexander and Goldspink, 1977; Full et al., 1991) has fostered a lack of interest in individual limb mechanics of quadrupeds and has even led to the development of quadrupedal robots with fore- and hindlegs that function identically. How would such a robot carry an asymmetrically distributed payload? Likewise, how would a tiger carry prey in its jaws or a pregnant wildebeest carry its fetus? In these examples, we expect that asymmetric loading will alter the fore–hind distribution of vertical force. This would be the only effect of asymmetrical loading if vertical and horizontal force components were independent. On the other hand, if the limbs functioned as struts, the horizontal force component would

change as a constant proportion of the vertical component. Asymmetrical loading also occurs due to the natural variation in antero–posterior body mass distribution amongst quadrupeds. It is difficult to imagine similar forelimb forces in hyenas and baboons, for instance. Here we propose that body mass distribution alters both the vertical and fore–aft forces exerted by the fore- and hindlimbs of trotting quadrupeds.

It is apparent that antero–posterior body mass distribution varies substantially amongst quadrupeds, yet this characteristic has been measured during standing in fewer than 20 species (Rollinson and Martin, 1981). In mammalian quadrupeds, the forelimbs typically support about 60% of body mass during standing, while the forelimbs of primates, lizards and alligators generally support less than 50%. Unfortunately, no data are available for quadrupeds with more extraordinary body types, such as giraffes and spotted hyenas, which appear to have extremely anterior center of mass positions, or rabbits, which appear to have extremely posterior center of mass positions.

We chose to study limb function during trotting because it

is the gait most commonly used by quadrupeds and it is a simple gait in which diagonal foot pairs are set down alternately. This facilitates comparison of individual forelimb and hindlimb function because diagonal fore- and hindfeet are set down in the same functional step. Trotting is unique in that the forelimb and hindlimb exert opposing fore–aft forces while in-phase with one another (Lee et al., 1999). The forelimb exerts a net braking force and the hindlimb exerts a net propulsive force during each trotting step. Although individual limb data from trotting quadrupeds are limited to cats, macaques, dogs, goats, horses and alligators (Demes et al., 1994; Kimura, 2000; Lee et al., 1999; Merkens et al., 1993; Pandy et al., 1988; Rumph et al., 1994; Willey et al., 2004), this phenomenon seems to be widespread in trotting animals. Opposing fore–aft force has also been reported in hexapedally trotting cockroaches, which exhibit primarily foreleg braking and hindleg propulsion (Full et al., 1991). This pattern reflects the substantial anterior inclination of the forelegs and posterior inclination of the hindlegs. In contrast, the mid-legs of cockroaches show no bias in limb angle and, accordingly, exert equal braking and propulsive force (Full et al., 1991).

In some cases, limbs act primarily as struts (Gray, 1968), such that minimal moments are exerted about their proximal joints. For example, the foreleg resultant force of trotting cockroaches tends to align closely with the leg axis (Full et al., 1991). On the other hand, strut action is sometimes accompanied by substantial lever action (Gray, 1968). For example, the strut action of the posteriorly inclined cockroach hindleg would exert higher propulsive force if not for the opposing lever action (i.e. proximal joint moment) tending to protract the hindleg (Full et al., 1991). During steady speed trotting, it would be advantageous for animals to use their limbs as springy struts, minimizing proximal joint moments and, thereby, increasing the overall economy of locomotion (Alexander, 1977).

We predicted that body mass distribution would affect the individual limb force patterns, and tested this idea by adding 10% body mass near the center of mass, at the pectoral girdle, or at the pelvic girdle of trotting dogs. Assuming that the limbs act as struts, a disproportionate increase in loading of either the fore- or hindlimb would increase both the vertical and fore–aft components of ground reaction force on that limb. Hence, in the absence of functional compensation, hindlimb propulsive force would tend to increase in response to pelvic girdle loading and forelimb braking force would tend to increase in response to pectoral girdle loading. Because braking and propulsion must be in equilibrium during steady speed trotting, compensatory changes in limb function, as evidenced by the b–p bias and relative contact time, would be expected during experimental loading of the limb girdles.

Materials and methods
Subjects and data collection

Five adult dogs (*Canis familiaris* L.) of various breeds were used in this experiment. Subjects ranged in body mass from

Table 1. *Subject descriptions*

Dog	Mass (kg)	Hip height (m)	Age (years)	Breed	Sex
A	29.5	0.545	8	Pointer/scent hound	M
B	34.5	0.573	2	German shepherd	M
C	23.5	0.525	5	Coonhound	M
D	33.1	0.556	9	German shepherd mix	M
E	31.6	0.498	2	Golden retriever	F

23.5 to 34.5 kg and from 2 to 9 years of age (Table 1). The dogs were borrowed from private owners for a period of 8 h or less and were never kept overnight. During data collection sessions, water was provided *ad libitum* and periodic rest breaks were given. The dogs trotted as they were led on a leash across a level, hard-packed soil runway in which two force platforms were positioned in series (Fig. 1A). This allowed independent measurement of simultaneous fore- and hindlimb ground reaction forces (Fig. 1B).

Data were collected while the dogs carried no load (unloaded, U) and under three loading conditions, in which tandem saddle bag packs were worn (Fig. 1A). Two small bags of lead shot totaling 10% body mass were inserted bilaterally in the anterior compartments of the pectoral pack (fore-loaded, F), the posterior compartments of the pectoral pack (mid-loaded, M), or the posterior compartments of the pelvic pack (hind-loaded, H). We tested four hypotheses. Loading at the limb girdles (conditions F and H) will (1) change the fore–hind distribution of vertical impulse during trotting, (2) decrease the braking–propulsive (b–p) bias of the loaded limb and (3) increase the relative contact time of the loaded limb. (4) Loading (conditions M, F and H) will *not* affect the weight-normalized mean fore–aft forces exerted individually by the fore- and hindlimb.

Force and center of pressure measurements

Force data were collected at 360 Hz from two strain gauge type force platforms (made by N. T. Heglund) positioned in series, using LabView™ software and a National Instruments™ (Austin, TX, USA) data acquisition system (DAQCard AI-16-E4, SCXI 1000 chassis, SCXI 1121 strain/bridge modules, and SCXI 1321 terminal blocks). Data were collected for 2 s as the dogs crossed the platforms. Only data from uninterrupted trotting were saved. Each force platform was 0.6 m long by 0.4 m wide. Using platforms of this length increased the likelihood that diagonal fore- and hindfeet would strike separate force platforms simultaneously. Trials in which foot placements did not meet this criterion were discarded. Furthermore, footfalls that struck the platform edges as evidenced by negative vertical force (i.e. a moment tending to lift the opposite end) were discarded. The force platforms measured vertical and fore–aft ground reaction force (GRF) with separate double-cantilever transducers at each corner post. Vertical GRF acting upward and fore–aft GRF acting in the direction of travel were considered positive. Vertical impulse
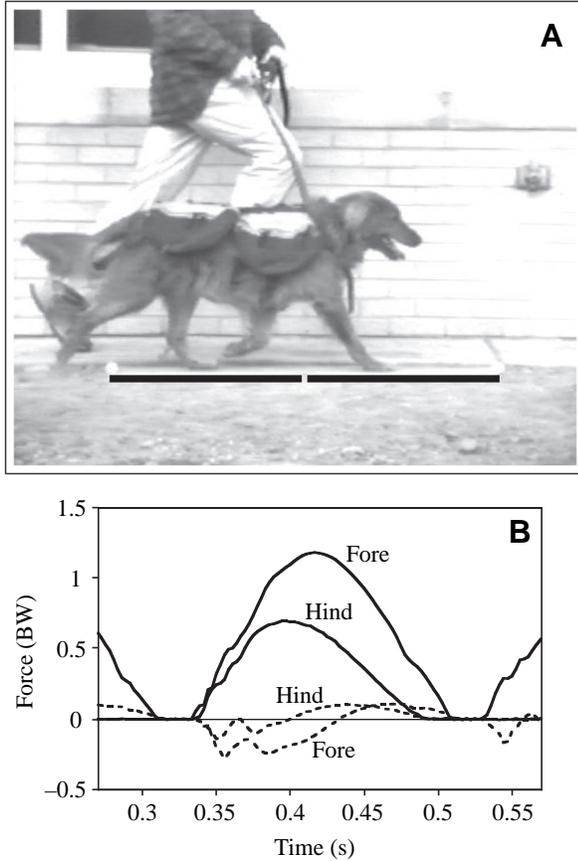
Fig. 1. (A) Simultaneous fore- and hindlimb supports were recorded by two separate force platforms (thick lines) during trotting. (B) Ground reaction forces were measured independently by the two force platforms. Solid lines indicate vertical force and broken lines fore–aft force. BW, body weight.

j_z and fore–aft impulse j_y were determined by numerical integration of GRF from an individual limb over the limb contact time ($t_{c,fore}$ or $t_{c,hind}$) or both diagonal limbs over the paired contact time $t_{c,total}$ of the diagonal limbs. A key to the notation used throughout this report is provided in Appendix A.

Normalized mean vertical force exerted on the center of mass during paired diagonal supports was determined by:

$$\overline{F}_z = (j_{z,total}/t_{c,total})/m\boldsymbol{g} , \tag{1}$$

where m is body mass (or 110% of body mass under loaded conditions) and $\boldsymbol{g}$ is gravitational acceleration. Likewise, normalized mean fore–aft acceleration of the center of mass, which is equivalent to force in dimensionless terms, was determined by:

$$\overline{A}_y = (j_{y,total}/t_{c,total})/m\boldsymbol{g} . \tag{2}$$

Normalized mean fore–aft force exerted separately on the forelimb and hindlimb during paired diagonal supports were determined by:

$$\overline{F}_{y,fore} = (j_{y,fore}/t_{c,total})/m\boldsymbol{g} , \tag{3}$$

and

$$\overline{F}_{y,hind} = (j_{y,hind}/t_{c,total})/m\boldsymbol{g} . \tag{4}$$

The mean angle of the resultant force vector during fore- or hindlimb contact was determined by:

$$\theta = \tan^{-1}(j_y/j_z) . \tag{5}$$

Forelimb vertical impulse was expressed as a fraction of total vertical impulse during paired diagonal supports. This quantity is referred to as the vertical impulse ratio:

$$R = j_{z,fore}/j_{z,total} , \tag{6}$$

(Jayes and Alexander, 1978; Lee et al., 1999).

In order to determine a limb's functional bias toward braking or propulsion, a Fourier method (Hamming, 1973) adapted to the analysis of force–time curves by Alexander and Jayes (1980) was used to quantify fore–aft force curve shape. This method decomposes a complex waveform into five simple sinusoids of progressively higher frequency (i.e. shape complexity). These sinusoids are known as Fourier terms and each term has a coefficient, the magnitude of which indicates its influence on the shape of the waveform. The five coefficients generated by this analysis are a_1, b_2, a_3, b_4 and a_5, where a indicates a cosine term and b, a sine term. The lower frequency terms a_1 and b_2 define the basic waveform, hence, by expressing a_1 as a fraction of b_2 (or *vice versa*), the waveform shape can be described in dimensionless terms (Alexander and Jayes, 1980). Here, a_1/b_2 was used to quantify fore–aft force curve shape, which is referred to as the braking–propulsive (b–p) bias. Force–curve shapes defined by negative and positive values of a_1/b_2 are shown in Fig. 2. Negative values indicate a braking bias, positive values indicate a propulsive bias, and zero indicates a symmetrical force curve with no bias toward braking or propulsion. In this study, the b–p bias (a_1/b_2) was computed from individual limb fore–aft force curves.

Center of pressure was measured in a conventional manner by comparing the vertical force from independent transducer elements at the fore and aft ends of a force platform. The two platforms were calibrated on a continuous metric scale to facilitate the computation of distance between supports on separate platforms (Bertram et al., 1997). Center of pressure position for each foot was determined by force-averaging over the duration of foot contact. In other words, instantaneous centers of pressure were weighted according to the
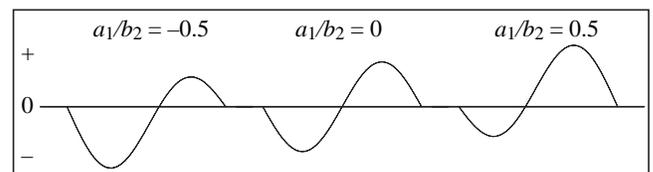

Fig. 2. Illustration of braking–propulsive biases defined by different values of the Fourier shape ratio a_1/b_2. $a_1/b_2 = -0.5$ indicates a braking bias, $a_1/b_2 = 0$ indicates no b–p bias, and $a_1/b_2 = 0.5$ indicates a propulsive bias.

instantaneous vertical force values, summed, and then divided by the summation of vertical force over the time of contact. This avoided the confounding effect of an extreme anterior foot position during toe-off, for example, when the vertical force is quite small. During paired diagonal contacts, the fore- and hindfeet struck separate platforms allowing calculation of the distance p between their mean center of pressure positions. The horizontal distance between fore- or hindlimb centers of pressure and a kinematic mid-point (described in the following section) was also determined.

Mean forward velocity $\bar{v}_{y,step}$ was determined directly from the force record by a method similar to that of Jayes and Alexander (1978), except that time and distance parameters were computed from vertical force peaks rather than initial foot contacts. The times t_{step} and distances d between subsequent forelimb supports and subsequent hindlimb supports were determined from the times of vertical force peaks and the corresponding center of pressure positions of each foot. Mean forward velocity $\bar{v}_{y,step}$ is the ratio of d to t_{step}. Because the paired diagonal supports of interest were preceded by a single forelimb support and followed by a single hindlimb support, forelimb and hindlimb values of $\bar{v}_{y,step}$, d_{step}, and t_{step} were averaged to provide the best estimates of these parameters. In order to account for size differences between dogs, mean velocity was expressed as a Froude number:

$$\text{Froude} = \bar{v}_{y,step}/\sqrt{gh}, \qquad (7)$$

where g is gravitational acceleration and h is hip height as defined in the following section. The aforementioned step period t_{step} is one half of the stride period during trotting. For consistency with existing literature, the stride period ($2t_{step}$) was used to normalize individual foot and paired diagonal contact times. The ratio of foot contact time to stride period is termed the duty factor DF and was computed as:

$$DF_{total} = t_{c,total}/2t_{step}, \qquad (8)$$

$$DF_{fore} = t_{c,fore}/2t_{step}, \qquad (9)$$

and

$$DF_{hind} = t_{c,hind}/2t_{step}. \qquad (10)$$

In addition, the ratio of fore- to hindlimb contact time $t_{c,f}/t_{c,h}$ was computed. The time of initial hindfoot contact with respect to initial forefoot contact was also expressed as a fraction of the stride period. This quantity, referred to as the hindlimb phase shift α_{hind}, was computed as:

$$\alpha_{hind} = (t_{i,hind} - t_{i,fore})/2t_{step}, \qquad (11)$$

where $t_{i,hind}$ and $t_{i,fore}$ are initial contact times. A negative value of α_{hind} indicates that hindlimb contact occurred before forelimb contact.

Videographic measurements

A video camera with VCR (PEAK™ Performance Technologies Inc., Centennial, CO, USA) acquired 120 images s⁻¹ in lateral view. Force and video acquisition were synchronized by connection of a manual switch to a PEAK™ Event Synchronization Unit, which simultaneously marked a video frame and triggered force acquisition *via* a breakout connector to the data acquisition card. The eye and the base of the tail were digitized in every other frame during paired diagonal contacts (i.e. $t_{c,total}$) and their mean horizontal (y) positions were computed. Then, the mean y-positions of the eye and the base of the tail were averaged to define a kinematic mid-point. This mid-point was used as a reference for the horizontal positions of the fore- and hindlimb centers of pressure with respect to the trunk. Finally, the vertical position of the base of the tail with respect to the substrate was used to approximate the mean hip height h during trotting, because it is near the greater trochanter (Table 1). Videographic measurements were taken from four approximately steady speed trials (i.e. $-0.04 \le \bar{A}_y \le 0.04$) for each dog under each loading condition.

Statistics

Comparisons between treatment conditions were made using either regression analysis or repeated measures ANOVA and Tukey–Kramer multiple comparison tests (InStat™ 2.0). The latter method was applied to mean vertical force, mean fore–aft acceleration, vertical impulse ratio, mean forward velocity and Froude number, as well as the distance between diagonal footfalls, p, and the distance between fore- or hind footfalls and the kinematic midpoint between the eye and base of the tail. For individual limb mean fore–aft force and b–p bias, which were functions of mean fore–aft acceleration, least-squares linear regression was used to compute the y-intercept (i.e. the steady speed condition) and its 95% confidence limits (Sokal and Rohlf, 1995). The regressions of $\bar{F}_{y,fore}$ and $\bar{F}_{y,hind}$ on $\bar{A}_y$ were linear, as was the regression of $a_1/b_{2,fore}$ on $\bar{A}_y$. The log transformation of $a_1/b_{2,hind}$ allowed the use of a linear regression to determine its steady speed value.

Values of other locomotor parameters were determined by simultaneously regressing the parameter of interest on mean fore–aft acceleration and mean forward velocity. If both multiple regression coefficients were significantly different from zero ($P<0.10$), the multiple regression equation was used to predict the steady speed value of the locomotor parameter. If only one regression coefficient was significantly different from zero ($P<0.10$), the non-significant independent variable was dropped from the model and least-squares linear regression was used to predict either the steady speed value of the locomotion parameter or its value at the appropriate mean velocity. In cases where both multiple regression coefficients were not significantly different from zero ($P>0.10$), the sampled mean of the locomotor parameter was reported.

Results

During paired diagonal supports, mean vertical ground reaction force $\bar{F}_z$ was greatest in the unloaded condition (Table 2A). The unloaded mean vertical force of 1.04 body weights (BW) was significantly ($P<0.05$) higher than that of

Table 2. *Mean vertical force, mean fore–aft acceleration and vertical impulse ratio*

Loading condition	Dog	$\bar{F}_z$ (BW)	$\bar{A}_y$ (BW)	R	R_0
(A)					
U	A	1.037	0.0037	0.663	0.665
U	B	0.987	0.0535	0.640	0.678
U	C	1.075	0.0248	0.658	0.676
U	D	1.055	−0.0155	0.626	0.615
U	E	1.027	0.0142	0.596	0.606
U	$\bar{X}$	**1.036±0.015**	**0.0161±0.0115**	**0.637±0.012**	**0.648±0.016**
M	A	0.998	−0.0330	0.693	0.670
M	B	0.927	0.0097	0.671	0.678
M	C	1.010	0.0200	0.684	0.698
M	D	1.004	0.0093	0.637	0.644
M	E	0.995	0.0042	0.617	0.619
M	$\bar{X}$	**0.987±0.015**	**0.0020±0.0091**	**0.660±0.015**	**0.662±0.014**
F	A	0.976	−0.0323	0.712	0.689
F	B	0.957	0.0050	0.682	0.685
F	C	0.999	0.0211	0.700	0.715
F	D	1.009	−0.0392	0.682	0.654
F	E	0.976	0.0023	0.629	0.631
F	$\bar{X}$	**0.983±0.009**	**−0.0086±0.0116**	**0.681±0.014**	**0.675±0.015**
H	A	1.013	0.0056	0.644	0.648
H	B	0.974	−0.0034	0.628	0.626
H	C	1.017	0.0158	0.629	0.640
H	D	1.004	−0.0101	0.591	0.584
H	E	1.005	0.0329	0.566	0.589
H	$\bar{X}$	**1.002±0.008**	**0.0082±0.0076**	**0.612±0.015**	**0.617±0.013**
(B)					
U *vs.* M		−0.049***	−0.0141[ns]	0.024**	0.014[ns]
U *vs.* F		−0.053***	−0.0248[ns]	0.044***	0.027**
U *vs.* H		−0.034**	−0.0080[ns]	−0.025***	−0.031**
M *vs.* F		−0.004[ns]	−0.0107[ns]	0.021**	0.013[ns]
M *vs.* H		0.016[ns]	0.0061[ns]	−0.049***	−0.044***
F *vs.* H		0.019[ns]	0.0168[ns]	−0.069***	−0.057***

$\bar{F}_z$, mean vertical force; $\bar{A}_y$, mean fore–aft acceleration; R, vertical impulse ratio; R_0, R at steady speed.

Sample means are given for each dog and loading condition (U, unloaded; M, mid-load; F, fore-load; H, hind-load).

BW, body weight, or 110% body weight during experimental loading.

See the text for parameter definitions.

(A) values are means for each dog and group means ± S.E.M. for each loading condition.

(B) Differences between means of each loading condition (e.g. 'U *vs.* M' was computed as $\bar{M}$–$\bar{U}$). Asterisks indicate the results of Tukey–Kramer tests comparing each loading condition to the others (***$P<0.001$, **$P<0.01$, *$P<0.05$, [ns]$P>0.05$).

the three loaded conditions, which were between 0.98 and 1.0 BW (Table 2B). Only the unloaded $\bar{F}_z$ was significantly different from one ($P<0.05$). Mean forward velocity $\bar{v}_{y,step}$ was, on average, higher in the unloaded than in the loaded conditions (U, 3.09 m s^{-1}; M, 2.81 m s^{-1}; F, 2.70 m s^{-1}; H, 2.77 m s^{-1}). These differences were significant ($P<0.05$) only in the F condition. When $\bar{v}_{y,step}$ was normalized as a Froude number (yielding treatment means between 1.17 and 1.35), the statistical comparisons between loading conditions were the same as before normalization. Velocity differences between unloaded and loaded conditions were taken into account by predicting locomotor parameters at an intermediate $\bar{v}_{y,step}$ of 2.86 m s^{-1} whenever a parameter was significantly ($P<0.10$) related to $\bar{v}_{y,step}$ (Table 3). This analysis produced statistically similar values of distance between subsequent footfalls d as well as step period t_{step} across all four loading conditions (U, M, F and H) (Table 4). Ground reaction forces reconstructed from locomotor parameters reported in this section and in Appendix B illustrate steady speed GRF patterns at 2.86 m s^{-1} for U, M, F and H conditions (Fig. 3).

Table 3. *Regression coefficients (±95% C.I.) for various parameters* versus *mean fore–aft acceleration and mean forward velocity*

Parameter	vs. $\bar{A}_y$ (BW)	vs. $\bar{v}_y$ (m s^{-1})	r^2
d (m)			
U	ns	0.111±0.021	0.58
M	ns	0.103±0.028	0.54
F	ns	0.095±0.032	0.35
H	–0.495±0.424	0.114±0.048	0.32
t_{step} (s)			
U	ns	–0.033±0.007	0.54
M	ns	–0.045±0.010	0.66
F	ns	–0.046±0.011	0.50
H	–0.163±0.146	–0.040±0.017	0.52
α_{hind}			
U	ns	ns	
M	ns	–0.046±0.032	0.16
F	ns	–0.042±0.023	0.17
H	ns	–0.042±0.034	0.11
DF_{total}			
U	ns	ns	
M	ns	–0.034±0.024	0.16
F	ns	–0.031±0.013	0.25
H	ns	–0.020±0.019	0.08
DF_{fore}			
U	ns	–0.027±0.022	0.07
M	ns	–0.049±0.025	0.26
F	ns	–0.047±0.016	0.35
H	ns	–0.052±0.023	0.29
DF_{hind}			
U	ns	–0.037±0.011	0.34
M	ns	–0.019±0.019	0.08
F	–0.224±0.144	ns	0.13
H	ns	–0.015±0.018	0.05
$t_{c,f}/t_{c,h}$			
U	ns	ns	
M	ns	ns	
F	0.871±0.723	–0.103±0.071	0.13
H	ns	–0.083±0.074	0.09
θ_{fore} (deg.)			
U	49.9±3.43	1.34±0.577	0.92
M	47.3±8.21	ns	0.75
F	50.4±8.94	ns	0.66
H	40.0±10.1	ns	0.56
θ_{hind} (deg.)			
U	56.6±6.79	–1.23±1.14	0.77
M	59.7±13.0	1.21±1.28	0.73
F	63.8±13.6	ns	0.57
H	71.7±14.3	ns	0.68

$\bar{A}_y$, mean fore–aft acceleration; $\bar{v}_y$, mean forward velocity.

Only significant ($P<0.10$) regression coefficients are shown (ns, not significant.)

U, unloaded; M, mid-load; F, fore-load; H, hind-load.
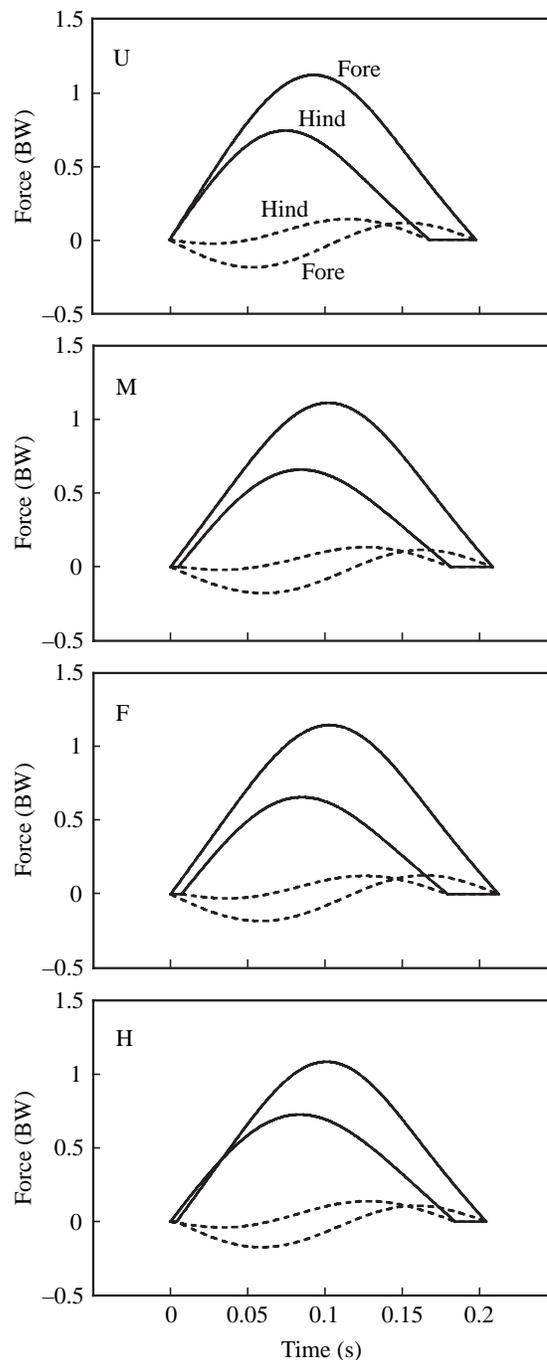
See the text for parameter definitions.

Fig. 3. Fore- and hindlimb force curves reconstructed from steady speed Fourier coefficients predicted at 2.86 m s^{-1} (see Materials and methods and Appendix B) for each of the loading conditions (U, unloaded; M, mid-load; F, fore-load; H, hind-load). Solid lines indicate vertical force and broken lines fore–aft force.

Mean fore–aft acceleration $\bar{A}_y$ was not significantly different between U, M, F and H conditions (Table 2). Nevertheless, substantial inter-subject variation was observed, with $\bar{A}_y$ individual means ranging from –0.039 to 0.054 BW. Thus, some dogs tended to speed up and others tended to slow down as they crossed the force platforms. Because the vertical

Table 4. *Steady speed locomotion parameters during level trotting at 2.86 m s^{-1} for each loading condition*

	Loading condition			
Parameter	U	M	F	H
d (m)	0.624±0.008	0.615±0.011	0.628±0.012	0.626±0.014
t_{step} (s)	0.219±0.003	0.217±0.004	0.222±0.004	0.220±0.005
α_{hind}	0.001±0.009	0.012±0.012	0.016±0.009*	−0.010±0.010*
DF_{total}	0.461±0.005	0.487±0.009*	0.485±0.005*	0.478±0.006*
DF_{fore}	0.451±0.009	0.476±0.009*	0.477±0.006*	0.455±0.007
DF_{hind}	0.383±0.004	0.405±0.007*	0.389±0.005*	0.418±0.006*
$t_{c,f}/t_{c,h}$	1.19±0.017	1.18±0.032	1.23±0.024*	1.09±0.022*
θ_{fore} (deg.)	−3.32±0.221	−3.43±0.307	−2.92±0.302*	−3.30±0.362
θ_{hind} (deg.)	5.84±0.438	6.46±0.454*	5.70±0.459	5.14±0.512*

Values are ±95% C.I.

Significant differences ($P<0.05$) from the unloaded condition are indicated by asterisks.

U, unloaded; M, mid-load; F, fore-load; H, hind-load.

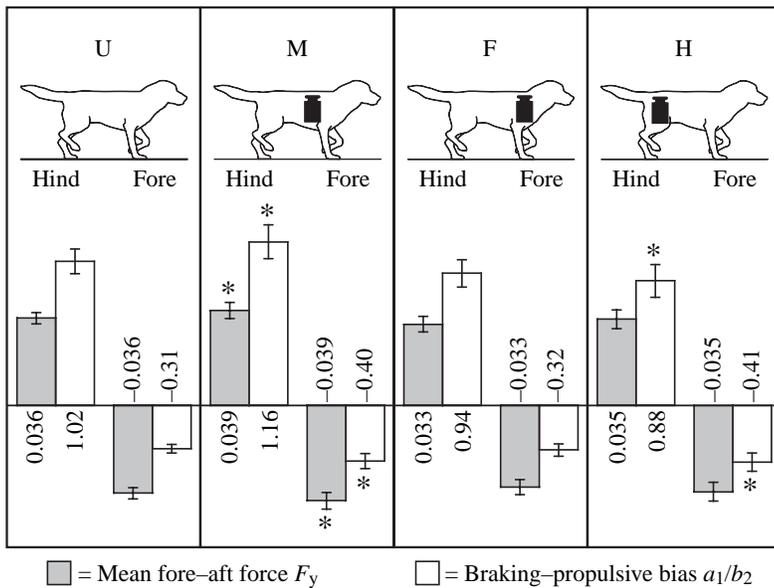See Appendix A and the text for parameter definitions.

Fig. 4. Steady speed values (±95% CI) of mean fore–aft force (filled bars) and braking–propulsive bias a_1/b_2 (open bars) for the loading conditions U, M, F and H (see text). Significant difference ($P<0.05$) from the unloaded condition U is indicated by an asterisk.

(Table 2B). In agreement with Hypothesis 1, F and H conditions significantly altered the fore–hind impulse distribution, while M maintained the natural impulse distribution.

In response to hind loading, $a_1/b_{2,hind}$ decreased significantly ($P<0.05$; from 1.02 to 0.88) with respect to U (Fig. 4). This reduction in propulsive bias is consistent with Hypothesis 2. Nonetheless, fore-loading did not significantly reduce forelimb braking bias (Fig. 4). In response to mid-loading, $a_1/b_{2,fore}$ decreased significantly ($P<0.05$) and $a_1/b_{2,hind}$ increased significantly ($P<0.05$) with respect to U. These unexpected increases in forelimb braking bias and hindlimb propulsive bias are considered in the Discussion.

Across all four conditions, $a_1/b_{2,hind}$ magnitude was, on average, 2.8 times that of $a_1/b_{2,fore}$ (Fig. 4). In the unloaded condition, for example, $a_1/b_{2,fore}$ was −0.31 and $a_1/b_{2,hind}$ was 1.02. Hence, the hindlimb showed a large propulsive bias and the forelimb, a relatively small braking bias. Similar patterns were observed in conditions M and F. However, the fore–hind difference in b–p bias became much less pronounced in response to hind-loading, such that hindlimb propulsive bias was only twice the forelimb braking bias (Fig. 4).

Like $a_1/b_{2,hind}$, the angle of the hindlimb resultant force θ_{hind} increased significantly ($P<0.05$) during mid-loading and decreased significantly ($P<0.05$) during hind-loading with respect to unloaded trotting, while it was statistically unchanged during fore-loading (Table 4). In contrast to

impulse ratio R is a linear function of $\overline{A}_y$, individual R values required adjustment to better predict the steady speed vertical impulse ratio R_0. This was done according to the functional relationship between R and $\overline{A}_y$, reported to be −0.71 in separate analyses of Labrador retrievers and greyhounds, which span a full range of R_0 from 0.56 to 0.64 (Lee et al., 1999). A discrete slope of the regression of R on $\overline{A}_y$ was not available from the present analysis due to disparity in body mass distribution associated with the use of various breeds. Hence, the regression coefficient of −0.71 was applied in the estimation of R_0:

$$R_0 = R + \overline{A}_y(-0.71) . \qquad (12)$$

Mean values of R and R_0 are reported for each subject in Table 2. R_0 was not significantly different between U and M, but fore-loading increased R_0 by 0.027 ($P<0.01$) and hind-loading decreased R_0 by 0.031 ($P<0.01$) with respect to U

$a_1/b_{2,\text{fore}}$, θ_{fore} increased significantly ($P<0.05$) during fore-loading but did not decrease significantly during mid-loading with respect unloaded trotting (Table 4).

In agreement with Hypothesis 3, the relative contact time of the forelimb $t_{c,f}/t_{c,h}$ increased significantly ($P<0.05$) during fore-loading and decreased significantly ($P<0.05$) during hind-loading (Table 4). During mid-loading, relative contact time was statistically unchanged ($P>0.05$) from the unloaded condition. Duty factors increased significantly ($P<0.05$) under all loading conditions, with the exception of DF_{fore} during hind-loading (Table 4).

Steady speed values of $\bar{F}_{y,\text{fore}}$ were negative (braking) and steady speed values of $\bar{F}_{y,\text{hind}}$ were positive (propulsive) under all conditions (Fig. 4, filled bars). By definition, braking and propulsion were of equal magnitude during steady speed trotting. In the unloaded condition, for example, the magnitude was 0.036 BW (i.e. 3.6% of body weight). In agreement with Hypothesis 4, loading conditions F and H were not significantly different from U. Nonetheless, mid-loading resulted in an unexpected, statistically significant increase in braking and propulsive magnitude to 0.039 BW ($P<0.05$) (Fig. 4).

During unloaded trotting, hindlimb phase shift α_{hind} was approximately zero, indicating simultaneous initial contacts of the forelimb and hindlimb. Values of α_{hind} were significantly greater ($P<0.05$) during fore-loading and significantly less ($P<0.05$) during hind-loading (Table 4). In other words, hindlimb contact was relatively later during fore-loading and relatively earlier during hind-loading. This pattern is illustrated in the GRF reconstructions of Fig. 3.

The distance between the supporting diagonal limbs p was statistically unchanged ($P>0.05$) across loading conditions, with means of U, 0.569 m; M, 0.569 m; F, 0.562 m; H, 0.538 m. Hence, the spacing of diagonal supports was similar in U, M and F, while reduced, but not quite significantly, in H. Position of the diagonal supports with respect to the kinematic midpoint between the eye and base of the tail, was also conserved across U, M and F conditions; however, a statistically significant ($P<0.05$) anterior shift of the hindfoot position was observed during hind-loading (Fig. 5). The hindlimb reached about 0.03 m further forward in the hind-loaded than in the unloaded condition.

Discussion

Experimental mass manipulations

Experimental loading of the pectoral and pelvic girdles increased the fraction of vertical impulse on the fore- and hindlimb, respectively, during trotting (Hypothesis 1). The steady speed vertical impulse ratios R_0 were 0.648 in the unloaded condition, 0.675 during fore-loading, and 0.617 during hind-loading. An idealized model, in which the mass is added directly above the supporting forefoot or hindfoot, would predict R_0 of 0.68 in the fore-loaded condition and 0.59 in the hind-loaded condition. The predicted value is quite close to the actual value in the fore-loaded condition, indicating a
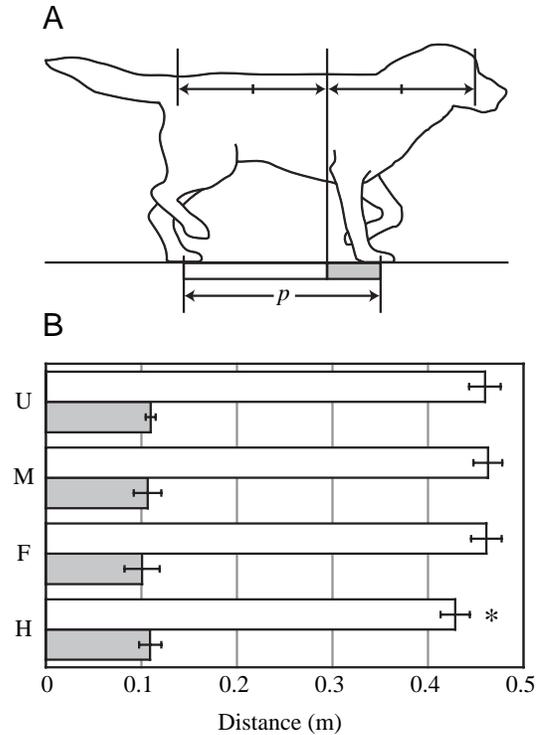

Fig. 5. (A) The kinematic mid-point between the eye and the base of the tail is represented by the vertical line posterior to the elbow. The distance p between hindlimb and forelimb centers of pressure was measured from force platform data and was partitioned according to this mid-point. (B) Distances from the mid-point to the hindlimb (open bars) and forelimb (filled bars) centers of pressure for the loading conditions U, M, F and H (see text). Error bars indicate 95% confidence intervals. Significant difference ($P<0.05$) from the unloaded condition U is indicated by an asterisk.

good alignment of the added mass with the forefoot. The predicted value is, however, smaller than the actual value in the hind-loaded condition, suggesting that the hindfoot was somewhat posterior to the added mass, which rested near the iliac crests. Experimental loading near the center of mass successfully maintained the natural distribution of vertical impulse between the fore- and hindlimb, as evidenced by the statistically similar R_0 of the unloaded and mid-loaded conditions.

The dogs tended to trot faster without an added load, but the difference in mean forward velocity was statistically significant only between the unloaded and fore-loaded conditions. Multiple regression of locomotor parameters on both mean fore–aft acceleration and mean forward velocity (Tables 3 and 4) allowed the computation of steady speed values at a common mean velocity of 2.86 m s^{-1}. This analysis removed the potentially confounding effects of subtle velocity differences between loading conditions. For example, the distance between subsequent footfalls d was greater in the unloaded than in the loaded conditions when simply comparing mean values, but multiple regression analysis revealed that d was similar across the four loading conditions

when compared at an intermediate speed of 2.86 m s^{-1} (Table 4). Furthermore, step period t_{step} was similar to unloaded values across loading conditions (Table 4). This result agrees well with published stride periods of loaded and unloaded trotting in horses carrying 14% body mass at 4.0 m s^{-1} (Sloet van Oldruitenborgh-Ooste et al., 1995) and in horses carrying 19% body mass at speeds above 3.0 m s^{-1} (Hoyt et al., 2000). In contrast to step period, duty factors were greater in the loaded conditions than in the unloaded condition. This agrees qualitatively with time of contact results from load-carrying experiments in trotting horses (Hoyt et al., 2000; Sloet van Oldruitenborgh-Ooste et al., 1995).

Effect of adding mass near the center of mass

On the basis that limbs act primarily as struts, we predicted that adding mass near the center of mass would *not* effect individual limb mean fore–aft force (normalized to body weight + added weight) (Hypothesis 4). Such a result was previously observed when mass was added near the center of mass of running humans, in which absolute braking and propulsive impulse components increased in direct proportion to the added weight (Chang et al., 2000). We also predicted that the individual limb b–p bias (i.e. the Fourier ratio a_1/b_2) would be affected by addition of mass at the limb girdles, but *not* when mass was added near the center of mass (Hypothesis 2). Nonetheless, both mean fore–aft force and b–p bias showed increased magnitudes in the mid-loaded condition with respect to the unloaded condition (Fig. 4). The magnitude of mean fore–aft force increased from 0.036 to 0.039 BW, while forelimb b–p bias decreased from –0.31 to –0.40 and hindlimb b–p bias increased from 1.02 to 1.16. This unexpected increase in both mean fore–aft force and b–p bias magnitudes has two potential explanations. The first is a change in limb excursions such that the forefoot would be positioned more anteriorly and the hindfoot, more posteriorly on average during stance. This would alter the mean fore–aft force and b–p bias due to the action of the limbs as struts with steeper antero–posterior inclinations. Alternatively, the mean fore–aft force and b–p bias could have been augmented by moments exerted by the protractor muscles of the shoulder and retractor muscles of the hip. Such a mechanism would constitute a classic example of action of the limbs as levers, as described by Gray (1968). In our experiments, a simple measurement of the horizontal distance p between simultaneous fore and hind supports showed that this distance was the same in the unloaded and mid-loaded conditions (Fig. 5). Hence, fore- and hindfoot positions could *not* have shifted in opposite directions. Forelimb protracting and hindlimb retracting moments must have been responsible for the observed changes in mean fore–aft force and b–p bias during mid-loading. Assuming a mean leg length of 0.54 m, both the shoulder and hip must have exerted additional mean moments of ±0.53 N m to produce the additional ±0.003 BW of mean fore–aft force measured during mid-loading.

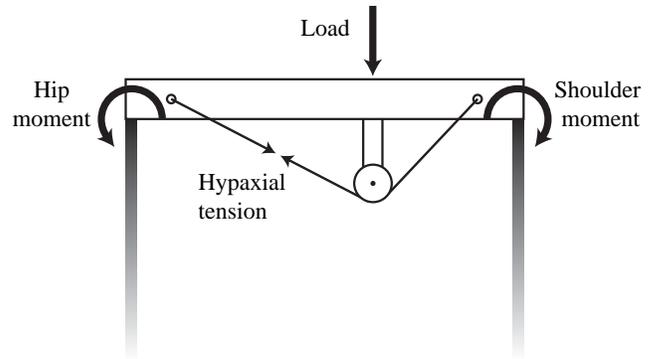Opposing shoulder and hip moments reveal important

Fig. 6. Trunk mechanics during trotting with a mid-trunk load. The load tends to ventroflex the trunk. Hindlimb retractors and forelimb protractors exert moments that tend to dorsiflex the trunk. Hypaxial muscle tension also tends to dorsiflex the trunk.

functional patterns when whole-body mechanics are considered. Although exerting opposing moments and fore–aft forces seems like a waste of metabolic energy, it may in fact be necessary to stabilize the trunk under certain circumstances. Gray (1968) hypothesized that simultaneous forelimb protracting and hindlimb retracting moments would exert an upward (dorsiflexing) bending moment on the trunk (Fig. 6). He argued that this mechanism could reduce the tension required in the hypaxial muscles that resist the downward (ventroflexing) bending moment due to gravity. This effect can be demonstrated easily with a flexible 15 cm ruler. Imagine holding the ruler face up with thumb and forefinger of each hand at its ends. The ruler will sag, or bend downward, under its own weight, putting the bottom surface of the ruler in tension. Now twist your palms upward – the resulting bending moment causes the ruler to bend upward, putting the top surface of the ruler in tension. The moments you applied to the ends of the ruler are analogous to the moments exerted on the trunk by the muscles of the shoulder and hip. If mass were added to the middle of the ruler, you would have to exert larger moments to bend the ruler upward. When mass is added at the center of mass of trotting dogs, our data show a compensatory increase of ±0.53 N m in shoulder and hip moments. Therefore, the shoulder plus hip moment contributing to upward bending of the trunk would be 1.06 N m.

By modeling the trunk as a beam rigidly fixed at its ends by the action of shoulder and hip muscles, one can determine the hip and shoulder moments required to maintain a net bending moment of zero across the length of the trunk. Estimating that the distance between the shoulder and hip was p (0.569 m) and that the added load of 0.1 BW (29.9 N) was applied at a distance $0.66p$ anterior to the hip, the required shoulder plus hip moment would be 3.8 N m. This suggests that the appendicular (i.e. shoulder and hip) muscles contributed just 28% of the moment required to balance the downward bending moment due to the added load. It is likely, however, that the remaining upward bending moment was imparted to the trunk by hypaxial muscles (Fig. 6). Because most hypaxials, such as

the rectus abdominis, act to bend the trunk upward, they could provide the additional bending moment required to support a mid-trunk load. In a previous study, such hypaxial action was evidenced by increased electrical activity in the internal oblique muscle of dogs trotting with mid-trunk loads (Fife et al., 2001). The use of appendicular muscles to exert a bending moment on the trunk is significant because it demonstrates a functional link between axial and appendicular mechanics. Gray's hypothesis aptly explains the observed effect of mid-loading on fore- and hindlimb mean fore–aft force and b–p bias.

Effect of adding mass at the pectoral girdle

We hypothesized that the loaded limb (the forelimb in this case) would show a decrease in b–p bias (Hypothesis 2). However, no statistically significant change in b–p bias was observed in either of the limbs during fore-loading. The forelimb braking bias was nearly identical in fore-loaded and unloaded conditions and the hindlimb propulsive bias showed a slight, insignificant decrease with respect to the unloaded value (Fig. 4). The fore- and hindlimb kinematics were similar in the fore-loaded and unloaded conditions, as evidenced by the distance between simultaneous fore and hind supports p and the distances of fore and hind supports from the mid-point between the eye and base of the tail (Fig. 5). Hence, during steady speed trotting, the forelimb may act as a strut with little or no antero–posterior inclination. This would explain the absence of a reduced braking bias in response to increased forelimb loading. As predicted (Hypothesis 4), mean fore–aft force was statistically unchanged from that of unloaded trotting.

In agreement with Hypothesis 3, the forelimb relative contact time $t_{c,f}/t_{c,h}$ increased from 1.19 (unloaded) to 1.23 during fore-loading (Table 4). This follows the same pattern observed in Labrador retrievers and greyhounds, which have substantially different antero–posterior body mass distributions. Although their hindlimb duty factors were statistically similar, Labrador retrievers (R_0=0.64) had forelimb duty factors of 0.505 and greyhounds (R_0=0.56) had forelimb duty factors of 0.426, a statistically significant difference ($P<0.05$; Bertram et al., 2000). Hence, a relatively high forelimb duty factor is naturally associated with a higher fraction of vertical impulse on the forelimb. We propose that, in general, relative fore- and hindlimb duty factors reflect the antero–posterior mass distributions of trotting quadrupeds. Biewener (1983) measured relative contact time of the forelimb in trotting mammals across a size range of 0.01 to 270 kg. At the trot–gallop transition speed, these ratios were less than 1.0 in mammals likely to support a larger fraction of body weight on their hindlimbs (i.e. pocket mouse, 0.88; mouse, 0.99; chipmunk, 0.96; ground squirrel, 0.95), but greater than 1.0 in mammals known to support more body weight on their forelimbs (i.e. dog, 1.07; pony, 1.04; horse, 1.01).

The fore-loaded condition also produced an unexpected change in the timing of foot placement. The phase shift of hindlimb initial contact increased from 0.001 (unloaded) to 0.016 during fore-loading, indicating that hindlimb was set down 1.5% of the stride period later in the fore-loaded condition (Fig. 3, Table 4). The same trend has been observed in Labrador retrievers and greyhounds, with hindlimb initial contact following forelimb initial contact in forelimb 'heavy' Labradors, but preceding forelimb initial contact in greyhounds (Bertram et al., 2000). Whether or not this pattern extends to other trotting quadrupeds is unknown.

Effect of adding mass at the pelvic girdle

Just as addition of mass at the pectoral girdle increased forelimb relative contact time ($t_{c,f}/t_{c,h}$), addition of mass at the pelvic girdle decreased forelimb relative contact time (i.e., increased hindlimb relative contact time). In agreement with Hypothesis 3, $t_{c,f}/t_{c,h}$ decreased from 1.19 (unloaded) to 1.09 during hind loading (Table 4). As predicted (Hypothesis 4), mean fore–aft force was unchanged from that of unloaded trotting (Fig. 4). The most prominent and functionally important difference between unloaded and hind-loaded trotting was the b–p bias. We predicted that the propulsive bias of the hindlimb would decrease in order to compensate for increased vertical impulse due to hind-loading (Hypothesis 2). This would prevent hindlimb propulsion from dominating forelimb braking. As expected, hindlimb propulsive bias decreased significantly from the unloaded value of 1.02 to 0.88 in the hind-loaded condition (Fig. 4). This compensatory change could have been achieved by decreasing the horizontal inclination of the hindlimb (strut action), decreasing the hindlimb retracting moment (lever action), or a combination of strut and lever action. From center of pressure data, it is clear that strut action could account for the decrease in propulsive bias. During hind-loading, the hindlimb center of pressure was significantly ($P<0.05$) more anterior than during unloaded trotting (Fig. 5). Given that this anterior shift was, on average, 0.03 m and the mean hindlimb length was 0.54 m, we know that the mean hindlimb angle was approximately 3.2° retracted with respect to the unloaded angle.

Without other changes in limb mechanics, a 3.2° change in mean limb angle would reduce propulsive force by 0.021 BW [i.e. 0.38 BW(tan3.2°)], which is seven times that required to compensate for the effect of hind-loading (i.e. 0.003 BW). The observed repositioning of the hindfoot would have reduced the mean fore–aft force by more than half without a hindlimb retracting moment to maintain the observed mean fore–aft force of 0.035 BW (Fig. 4). Given a fore–aft force deficit of 0.018 BW (i.e. 0.021–0.003) and a limb length of 0.54 m, the mean hindlimb retracting moment would need to be 2.9 N m, about three times that exerted by the shoulder plus hip during mid-loading. During hind-loading, the pelvis itself seems to have behaved much like a cantilever beam, supported primarily at the hip (posterior pelvis) while mass was added at the iliac crests (anterior pelvis). We conclude that the observed changes in the partitioning of hindlimb strut and lever action were largely due to local effects of loading the pelvis. If the added mass were applied 0.10 m anterior to the
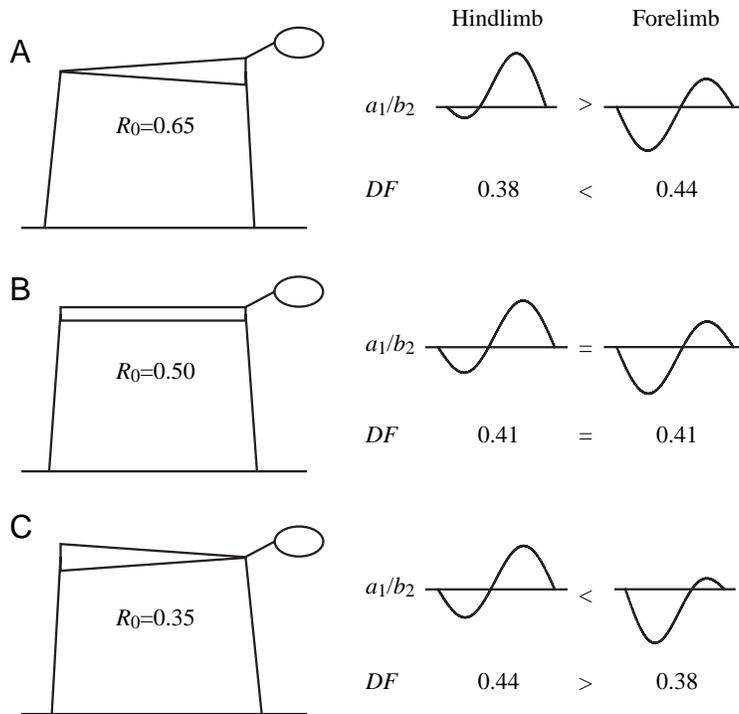
hip joint, a hindlimb retractor moment of 2.9 N m would be required to balance its effect. This is consistent with the actual placement of the added mass near the iliac crests. In contrast to mid-loading, the applied moment appears to have been resisted primarily by the hip muscles instead of being distributed between the shoulder, hip and, presumably, the trunk muscles.

Finally, the forelimb braking bias increased from the unloaded value of –0.31 to –0.41 in the hind-loaded condition (Fig. 4). The slight, statistically insignificant, anterior movement of the forefoot and/or an increase in forelimb protracting torque might have contributed to the observed increase in braking bias.

Implications for other quadrupeds

The axial and appendicular musculoskeletal systems of quadrupeds are designed to accommodate specific antero–posterior mass distributions. In this sense, the experimental addition of mass at discrete points seems unnatural. A load concentrated at the center of mass, pectoral girdle, or pelvic girdle is certainly not equivalent to the mass distributions inherent to different structural designs. An artificial load is, however, equivalent in one basic respect – its effect on the center of mass position. Based upon the assumption that limbs act primarily as struts, we hypothesized that a shift in antero–posterior mass distribution would alter individual limb mechanics. For example, the hindlimb propulsive bias decreased and its relative contact time increased in the hind-loaded condition. We propose that this relationship between antero–posterior mass distribution and limb function represents a general trend in trotting

quadrupeds. For example, trotting dogs (R_0=0.64) show a hindlimb propulsive bias approximately three times greater than the forelimb braking bias and a hindlimb duty factor 15% smaller than that of the forelimb. Cheetahs (*Acinonyx jubatus*, $R_0 \approx 0.52$; Kruger, 1943), which have more symmetric fore–hind weight distributions, are predicted to show approximately equal fore- and hindlimb b–p biases and duty factors. Lizards, which support more weight on their hindlimbs, are predicted to show greater forelimb braking biases and reduced forelimb duty factors relative to the hindlimb. This general pattern is illustrated in Fig. 7, which summarizes our results from trotting dogs and, based on these data, makes predictions for hypothetical quadrupeds with different fore–hind mass distributions.

As shown in Fig. 7A,C, the limb that supports a greater fraction of total vertical impulse is expected to have a greater duty factor and a b–p bias closer to zero. The limb that supports a smaller fraction of total vertical impulse is expected to have a smaller duty factor and, due to its reduced vertical force and contact time, is expected to compensate with a greater b–p bias. These duty factor predictions are also consistent with the tendency of more heavily loaded limbs to be relatively longer.

Individual limb forces have been reported for only a handful of trotting quadrupeds. Although most of these data represent trotting with substantial net braking, the results generally support the pattern of limb function illustrated in Fig. 7. In Dutch warmblood horses, Merkens and coworkers (Merkens et al., 1993) reported a vertical impulse ratio of 0.55 and a b–p bias similar to that of Fig. 7B. There was a small mean braking force of –0.014 BW, on average, in their sample of trotting steps. In cats, forelimb peak vertical force was found to be 1.69 times that of the hindlimb (Demes et al., 1994), which suggests a vertical impulse ratio between 0.60 and 0.70 during trotting. The same study showed that forelimb braking impulse was 3.5 times forelimb propulsive impulse and hindlimb propulsive impulse was 2.7 times hindlimb braking impulse, indicating a larger b–p bias in the forelimb. This pattern seems unusual in light of Fig. 7A, but is consistent with the mean net braking acceleration of –0.037 BW in their sample of trotting steps. The mean fore–aft forces exerted by the forelimb (–0.068 BW) and hindlimb (0.031 BW) of trotting cats are quite similar to those predicted for greyhounds trotting with a net braking acceleration of –0.037 BW (i.e. –0.070 and 0.033 BW, respectively; Lee et al., 1999).

Even fewer trotting data are available from quadrupeds with vertical impulse ratios below 0.50. Although individual limb function has been described in at least ten primate species (Demes et al., 1994), most primates use asymmetrical running gaits at higher speeds (Hildebrand, 1967). Nonetheless, Kimura (2000) has collected fast trotting data from adult Japanese macaques *Macaca fuscata*. He reported a vertical impulse ratio of 0.47, which is nearly equal to his measurement of standing weight distribution (0.46; Kimura et al., 1979). This is surprising, given that Kimura's sample of trotting steps represented a mean net braking acceleration of more than –0.10 BW, on average (Kimura, 2000). In trotting dogs, this degree of braking would cause a substantial increase in vertical impulse ratio (e.g. from 0.64 to 0.71 in Labradors; Lee et al., 1999). It is possible that macaques use a mechanism, such as forward foot placement (Raibert, 1990), to avoid a nose-down pitching moment (and subsequent vertical impulse redistribution) due to net braking. Because forelimb braking impulse was 11.1 times forelimb propulsive impulse and hindlimb propulsive impulse was roughly equal to hindlimb braking impulse, Kimura's data suggest a b–p bias similar to that of Fig. 7C. It is likely, however, that steady speed trotting of macaques is more like Fig. 7B.

Some mammals with extreme antero–posterior mass distributions, such as giraffes, hyenas and rabbits, have abandoned trotting and pacing gaits in favor of galloping and bounding gaits (Estes, 1993; Howell, 1944; Pennycuick, 1975). This may also be the case for some primates (Demes et al., 1994; Schmitt and Lemelin, 2002). Given that dogs (R_0=0.64) have a fairly extreme hindlimb propulsive bias, a more anterior center of mass position, such as that of hyenas, may exceed a limit by which propulsive impulse can be supplied by increasing hindlimb propulsive bias. Because hindlimb propulsive and forelimb braking impulses must be equal in magnitude during steady speed trotting steps, extreme antero–posterior mass distributions might favor galloping and bounding over trotting and pacing.

Although forelimb and hindlimb mechanics should generally accommodate a particular antero–posterior mass distribution, an individual's body mass distribution often changes in response to behavioral or physiological factors. Male cervids grow substantial masses at the end of a long neck every spring and then discard this mass in the autumn. The 'Irish elk' *Megaloceros giganteus*, with 40 kg antlers estimated to be approximately 7% body mass, provides a dramatic example (Geist, 1987). Carnivores can carry heavy prey in their jaws for some distance before consuming it. For example, man-eating tigers have been reported to run while carrying an intact human in their jaws (Corbett, 1946). Gray wolves *Canis lupus* often gorge on meals as large as 20–30% of their body mass, yet they may subsequently travel a few miles to find a suitable spot to rest (Mech, 1970). After making a kill and gorging as much as possible, African hunting dogs *Lycaon pictus* may need to escape from large scavengers such as

spotted hyenas or lions or, in other cases, chase a lone hyena from their kill at high speed (Creel and Creel, 2002). The most ubiquitous natural increase in trunk loading occurs in gravid females, which often carry substantial loads over periods of weeks or months. For example, neonatal mass is approximately 15% of maternal mass in the pronghorn and springbok (Robbins and Robbins, 1979). This value neglects the masses of the amniotic fluid and placenta, however, which are likely to be substantial. The distribution of fetal and placental mass is generally posterior to the center of mass in quadrupeds.

Conclusions

Adding mass to the pectoral or pelvic girdles significantly altered the fore–hind vertical impulse distribution of trotting dogs. Assuming that the limbs act as struts, we predicted that these changes would lead to a decrease in b–p bias and an increase in relative contact time of the experimentally loaded limb, while mean fore–aft force would be unaffected. All three of these predicted results were observed in the hind-loaded condition. Only the latter two were observed in the fore-loaded condition, perhaps due to a smaller initial b–p bias and/or limb inclination of the forelimb. We propose that the observed relationships between antero-posterior mass distribution, b–p bias, and relative contact time will apply to other quadrupeds. Our data also show that the mechanical effects of adding mass to the trunk are much more complex than would be predicted from center of mass position alone. During mid-loading, the shoulder and hip moments increased in order to resist the downward bending moment applied to the trunk. During hind-loading, the hindlimb retractor muscles exerted a large moment about the hip to resist the moment applied to the pelvis. In accordance with the pioneering models proposed by Sir James Gray (1968), both of these results exemplify a link between appendicular and axial mechanics *via* action of the limbs as levers.

Appendix A

$\bar{F}_z$	Dimensionless mean vertical force
$\bar{F}_y$	Dimensionless mean fore–aft force
$\bar{A}_y$	Dimensionless mean fore–aft acceleration
θ	Angle of the resultant force vector (degrees)
R	Vertical impulse ratio
R_0	Steady speed vertical impulse ratio
p	Distance between diagonal foot centers of pressure (m)
d	Distance between fore- and hindlimb centers of pressure of adjacent steps (m)
t_c	Time of contact (s)
t_{step}	Time between fore- and hindlimb vertical force peaks of adjacent steps (s)
$\bar{v}_{y,step}$	Mean forward velocity (m s^{-1})
DF	Duty factor
α_{hind}	Hindlimb phase shift

Appendix B

Steady speed Fourier coefficients during level trotting at 2.86 m s^{-1}

Vertical force curves

	$a_{1,\text{fore}}$ (BW)	$b_{2,\text{fore}}$ (BW)	$a_{3,\text{fore}}$ (BW)
U	1.06±0.02	–0.071±0.014	0.051±0.008
M	1.05±0.03	–0.025±0.015*	0.061±0.013
F	1.08±0.02	–0.041±0.011*	0.064±0.012*
H	1.02±0.03*	–0.039±0.015*	0.062±0.011
$\bar{X}$	**1.05**	**–0.044**	**0.060**

	$a_{1,\text{hind}}$ (BW)	$b_{2,\text{hind}}$ (BW)	$a_{3,\text{hind}}$ (BW)
U	0.708±0.016	–0.079±0.008	0.019±0.003
M	0.640±0.010*	–0.060±0.011*	0.010±0.006*
F	0.636±0.015*	–0.058±0.010*	0.013±0.004*
H	0.706±0.021	–0.060±0.010*	0.011±0.006*
$\bar{X}$	**0.673**	**0.064**	**0.013**

Fore–aft force curves

	$a_{1,\text{fore}}$	$b_{2,\text{fore}}$	$a_{3,\text{fore}}$
U	–0.052±0.004	0.149±0.005	–0.002±0.005
M	–0.055±0.006	0.143±0.006	–0.012±0.004*
F	–0.045±0.005*	0.153±0.005	–0.007±0.004
H	–0.050±0.007	0.139±0.006*	–0.004±0.005
$\bar{X}$	**–0.051**	**0.146**	**–0.006**

	$a_{1,\text{hind}}$	$b_{2,\text{hind}}$	$a_{3,\text{hind}}$
U	0.087±0.005	0.075±0.004	0.004±0.003
M	0.085±0.005	0.069±0.005*	0.002±0.004
F	0.073±0.006*	0.070±0.003*	0.004±0.003
H	0.076±0.007*	0.083±0.006*	0.005±0.005
$\bar{X}$	**0.080**	**0.074**	**0.004**

Values are ± 95% C.I. for each loading condition and overall means are shown.

Significant differences ($P<0.05$) from the unloaded condition are indicated by asterisks.

U, unloaded; M, mid-load; F, fore-load; H, hind-load.

For an explanation of the Fourier coefficients a_1, a_2 and b_2, see Materials and methods.

References

Alexander, R. M. (1977). Mechanics and scaling of terrestrial locomotion. In *Scale Effects in Animal Locomotion*: based on the proceedings of an international symposium held at Cambridge University, September, 1975 (ed. T. J. Pedley), pp. 93-110. London: Academic Press.

Alexander, R. M. and Goldspink, G. (1977). *Mechanics and Energetics of Animal Locomotion*. London, New York: Chapman and Hall. Distributed by Halsted Press.

Alexander, R. M. and Jayes, A. S. (1980). Fourier analysis of forces exerted in walking and running. *J. Biomech.* **13**, 383-390.

Bertram, J. E. A., Lee, D. V., Case, H. N. and Todhunter, R. J. (2000). Comparison of the trotting gaits of Labrador Retrievers and Greyhounds. *Am. J. Vet. Res.* **61**, 832-838.

Bertram, J. E. A., Lee, D. V., Todhunter, R. J., Foels, W. S., Williams, A. and Lust, G. (1997). Multiple force platform analysis of the canine trot: a new approach to assessing basic characteristics of locomotion. *Vet. Comp. Orthoped. Traumatol.* **10**, 160-169.

Biewener, A. A. (1983). Allometry of quadrupedal locomotion: the scaling of duty factor, bone curvature and limb orientation to body size. *J. Exp. Biol.* **105**, 147-171.

Chang, Y. H., Huang, H. W., Hamerski, C. M. and Kram, R. (2000). The independent effects of gravity and inertia on running mechanics. *J. Exp. Biol.* **203**, 229-238.

Corbett, J. (1946). *Man-eaters of Kumaon*. New York: Oxford University Press.

Creel, S. and Creel, N. M. (2002). *The African Wild Dog: Behavior, Ecology, and Conservation*. Princeton, N.J.: Princeton University Press.

Demes, B., Larson, S. G., Stern, J. T. J., Jungers, W. L., Biknevicius, A. R. and Schmitt, D. (1994). The kinetics of primate quadrupedalism: 'hindlimb drive' reconsidered. *J. Hum. Evol.* **26**, 353-374.

Estes, R. (1993). *The Safari Companion: A Guide to Watching African Mammals: Including Hoofed Mammals, Carnivores, and Primates*. Post Mills, Vt.: Chelsea Green.

Fife, M. M., Bailey, C. L., Lee, D. V. and Carrier, D. R. (2001). Function of the oblique hypaxial muscles in trotting dogs. *J. Exp. Biol.* **204**, 2371-2381.

Full, R. J., Blickhan, R. and Ting, L. H. (1991). Leg design in hexapedal runners. *J. Exp. Biol.* **158**, 369-390.

Geist, V. (1987). On the evolution of optical signals in deer: a preliminary analysis. In *Biology and Management of the Cervidae* (ed. C. M. Wemmer), pp. 235-255. Washington: Smithsonian Institution Press.

Gray, J. (1968). *Animal Locomotion*. New York: Norton.

Hamming, R. W. (1973). *Numerical Methods for Scientists and Engineers*. New York: McGraw-Hill.

Hildebrand, M. (1967). Symmetrical gaits of primates. *Am. J. Phys. Anthropol.* **26**, 119-130.

Howell, A. B. (1944). *Speed In Animals; Their Specialization for Running and Leaping*. Chicago: University of Chicago Press.

Hoyt, D. F., Wickler, S. J. and Cogger, E. A. (2000). Time of contact and step length: the effect of limb length, running speed, load carrying and incline. *J. Exp. Biol.* **203**, 221-227.

Jayes, A. S. and Alexander, R. M. (1978). Mechanics of locomotion of dogs (*Canis familiaris*) and sheep (*Ovis aries*). *J. Zool.* **185**, 289-308.

Kimura, T. (2000). Development of quadrupedal locomotion on level surfaces in Japanese macaques. *Folia Primatol (Basel)* **71**, 323-333.

Kimura, T., Okada, M. and Ishida, H. (1979). Kinesiological characteristics of primate walking: its significance in human walking. In *Environment, Behavior and Morphology: Dynamic Interactions in Primates* (ed. M. E. Morbeck, H. Preuschoft and N. Gomberg), pp. 297-311. New York: Gustav Fischer.

Kruger, W. (1943). Uber die beziehungen zwischen schwerpunktslage und starke der substantia compacta einzelner gliedmabenkochen bei vierfubigen saugetieren. *Morphol. Jahrb.* **88**, 377-396.

Lee, D. V., Bertram, J. E. A. and Todhunter, R. J. (1999). Acceleration and balance in trotting dogs. *J. Exp. Biol.* **202**, 3565-3573.

Mech, L. D. (1970). *The Wolf: The Ecology and Behavior of an Endangered Species*. Garden City, NY: Published for the American Museum of Natural History by the Natural History Press.

Merkens, H. W., Schamhardt, H. C., Van Osch, G. J. and Van den Bogert, A. J. (1993). Ground reaction force patterns of Dutch warmblood horses at normal trot. *Equine Vet. J.* **25**, 134-137.

Pandy, M. G., Kumar, V., Berme, N. and Waldron, K. J. (1988). The dynamics of quadrupedal locomotion. *J. Biomech. Eng.* **110**, 230-237.

Pennycuick, C. J. (1975). On the running of the gnu (*Connochaetes taurinus*) and other species. *J. Exp. Biol.* **63**, 775-799.

Raibert, M. H. (1990). Trotting, pacing and bounding by a quadruped robot. *J. Biomech.* **23 Suppl. 1**, 79-98.

Robbins, C. T. and Robbins, B. L. (1979). Fetal and neonatal growth patterns

and maternal reproductive effort in ungulates and subungulates. *Am. Nat.* **114**, 101-116.

Rollinson, J. and Martin, R. D. (1981). Comparative aspects of primate locomotion with special reference to arboreal cercopithecines. *Symp. Zool. Soc. Lond.* **48**, 377-427.

Rumph, P. F., Lander, J. E., Kincaid, S. A., Baird, D. K., Kammermann, J. R. and Visco, D. M. (1994). Ground reaction force profiles from force platform gait analyses of clinically normal mesomorphic dogs at the trot. *Am. J. Vet. Res.* **55**, 756-761.

Schmitt, D. and Lemelin, P. (2002). Origins of primate locomotion: gait mechanics of the woolly opossum. *Am. J. Phys. Anthropol.* **118**, 231-238.

Sloet van Oldruitenborgh-Ooste, M. M., Barneveld, A. and Schamhardt, H. C. (1995). Effects of weight and riding on work load and locomotion during treadmill exercise. *Equine Vet.* J. **18**, 413-417.

Sokal, R. R. and Rohlf, F. J. (1995). *Biometry: The Principles and Practice of Statistics in Biological Research*. New York: Freeman.

Willey, J. S., Biknevicius, A. R., Reilly, S. M. and Earls, K. D. (2004). The tale of the tail: Limb function and locomotor mechanics in *Alligator mississippiensis. J. Exp. Biol.* **207**, 553-563.